Theoretical study of expanded selenium in the supercritical region

1998 J. Phys.: Condens. Matter 10 11419

(http://iopscience.iop.org/0953-8984/10/49/028)

J. Phys.: Condens. Matter **10** (1998) 11419–11428. Printed in the UK PII: S0953-8984(98)96503-1

Theoretical study of expanded selenium in the supercritical region

Fumiko Yonezawa†§, Hiroaki Ohtani† and Toshio Yamaguchi‡

† Department of Physics, Keio University, 3-14-1 Hiyoshi, Kohoku-ku, Yokohama 223-8522, Japan

‡ Department of Physics, Tokyo Women's Medical College, 8-1 Kawadacho, Shinjuku-ku, Tokyo 162-8666, Japan

Received 4 June 1998

Abstract. By means of theoretical calculations, we elucidate the mechanism for the nonmetal-to-metal (NM-to-M) transition that occurs with density decrease in supercritical Se. We first show from energetical considerations that some of the bonds in Se chains are disrupted when the density is decreased, and secondly we clarify that the bond disruption causes a drastic reduction of the splitting ($E_{\sigma^*-\sigma}$) between the bonding (σ) and anti-bonding (σ^*) levels. As a consequence, the energy gap separating occupied and unoccupied levels decreases and eventually disappears, thus altering the nature of the system from nonmetallic to metallic. A remarkable point is that, although the bandwidth (W) reduces on decrease of the density, the degree of the reduction in $E_{\sigma^*-\sigma}$ is so marked that the ratio ($W/E_{\sigma^*-\sigma}$) *increases*. This feature is in contrast with the traditional Wilson transition, in which the decrease of density has no significant influence on the differences between the corresponding energy levels, such as the spacing between the s level and the p level in the case of expanded Hg, while the decrease of the density narrows the bandwidth W and reduces the ratio $W/E_{\sigma^*-\sigma}$ as well, and accordingly a metal-to-nonmetal transition is induced. Our calculations also show that structural changes such as shortening of the bond lengths take place at the NM-to-M transition.

1. What is the problem?

To date, several mechanisms for metal–nonmetal (M–NM) transitions have been proposed, such as those listed in the first four rows of table 1. In the Wilson transition, the opening of bands consequent upon the density decrease of the constituent atoms leads to a metal-to-nonmetal (M-to-NM) transition. Electron correlation also plays a part in M–NM transitions, which are often known by different names, the most common of which is 'Mott transitions'. In a system where electron correlation is important, a M-to-NM transition is expected to take place when the relative magnitude of the electron correlation exceeds the bandwidths as a result of the density decrease. The Peierls transition appears when the periodicity of a system is changed. The Anderson transition is found in random systems. A M-to-NM transition of this type is observed when the bandwidths fall below the degree of randomness accompanying the density decrease.

In all of the mechanisms known so far, the effect of the density decrease is manifested in the narrowing of the relevant bands, and, as a consequence, a M-to-NM transition. The situation is sketched in figure 1. Some examples of M-to-NM transitions are observed in

§ Author to whom any correspondence should be addressed.

0953-8984/98/4911419+10$19.50

Table 1. Mechanisms for the metal–nonmetal (M–NM) transition.

			Density ↘			
	M–NM transition	Mechanism	Band-width	Characteristic quantity	Ratio	Transition
1	Wilson transition	Band broadening or narrowing	W ↘	$E_{ij} \sim$ constant	$\left(\frac{W}{E_{ij}}\right) \searrow$	
2	Mott–Hubbard transition	Electron correlation	W ↘	$U \sim$ constant	$\left(\frac{W}{U}\right) \searrow$	M ⇒ NM
3	Anderson transition	Randomness	W ↘	$\Gamma \sim$ constant	$\left(\frac{W}{\Gamma}\right) \searrow$	
4	Peierls transition	Change in periodicity				
5	The present transition	Bond destruction	W ↘	$[E(\tilde{\sigma}^*) - E(\sigma)] \Downarrow$	$\left[\frac{W}{E(\tilde{\sigma}^*) - E(\sigma)}\right] \nearrow$	NM ⇒ M

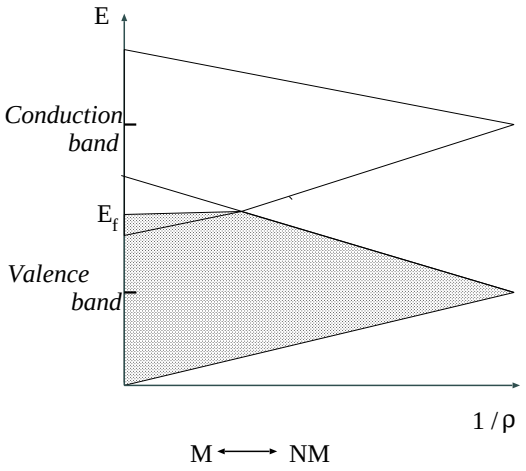

Figure 1. A schematic illustration of the band-widths as related to the density decrease.

the supercritical region of such metals as Hg (the Wilson transition) and alkali metals (the Mott transition). The situation is illustrated in figure 2(a).

On the other hand, a completely opposite case was found experimentally for expanded Se, where the decrease of the density brings about a nonmetal-to-metal (NM-to-M) transition instead of a M-to-NM transition. The situation is illustrated in figure 2(b), in which a NM-to-M transition is presented in which liquid Se is expanded by increasing the temperature along the rightward long arrow. This result is very surprising in the sense that the situation is in contradiction with the established understanding. It is the purpose of this article to resolve this problem [1].

Recently, Tamura and collaborators carried out an extensive study of expanded Se in the supercritical region by means of measurements of x-ray diffraction, the x-ray absorption fine structure (XAFS), and the extended x-ray absorption fine structure (EXAFS) [2–5].

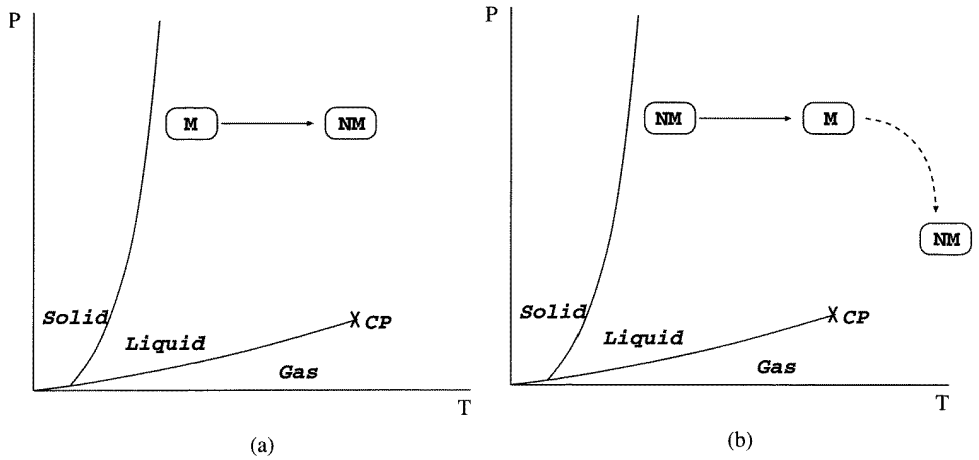

Figure 2. A schematic illustration of the experimental results in the pressure–temperature (P–T) space in the case of (a) Hg and alkali metals and (b) Se.

Their experimental results suggest that the chain structure is disrupted at high temperatures. This tendency has also been observed by computer simulations due to Bichara *et al* [6], Hohl and Jones [7], Kirchhoff *et al* [8, 9] and Shimojo *et al* [10].

The essential aspects of the experimental results can be summarized as follows.

(i) When the temperature of liquid Se is raised from T_m to temperatures near T_c at a fixed pressure which is higher than P_c, the density ρ decreases, and, accompanying this decrease of ρ, there is an increase of the conductivity σ. As a consequence, the system transforms from a nonmetallic (or semiconducting) to a metallic state as shown in figure 2(b). The measurements of the absorption edge lend support to the conductivity experiments.

(ii) X-ray diffraction, XAFS and EXAFS experiments all indicate that the nearest-neighbour distance r_1 (which is identical to the bond length) is about 2.32 Å in a nonmetallic (semiconducting) state while it is about 2.27 Å in a metallic state, the former being larger than the latter. It is worth mentioning here that the bond length in trigonal crystal is 2.38 Å.

(iii) The NMR measurement provides the number of unpaired spins in the system, from which it is implied that the chain length just above the melting curve is of order 10^5 while it is of order 10 in the supercritical region [11].

2. What is the method that we use?

In our calculations of the eigenvalues, we use the following method.

The density functional theory [12] reduces the calculation of the total energy for a system of interacting electrons to the solution of a single-particle equation of the form [13]

$$\left[-\frac{1}{2}\nabla^2 + \Phi(\boldsymbol{r}) + V_{\mathrm{ext}}(\boldsymbol{r}) + V_{\mathrm{xc}}(\boldsymbol{r})\right]\psi_i(\boldsymbol{r}) = \epsilon_i\psi_i(\boldsymbol{r}) \tag{1}$$

where $\psi_i(\boldsymbol{r})$ is the Kohn–Sham wave function for the single electron in the ith state, ϵ_i is the corresponding eigenvalue, $\Phi(\boldsymbol{r})$ is the Coulomb potential, $V_{\mathrm{ext}}(\boldsymbol{r})$ is the external potential of the nuclei, and $V_{\mathrm{xc}}(\boldsymbol{r}) \equiv \delta E_{\mathrm{xc}}/\delta n(\boldsymbol{r})$ is the exchange–correlation potential. The Coulomb potential $\Phi(\boldsymbol{r})$ and the exchange–correlation potential $V_{\mathrm{xc}}(\boldsymbol{r})$ are determined by

the density

$$n(\boldsymbol{r}) = \sum_i f_i |\psi_i(\boldsymbol{r})|^2 \tag{2}$$

where f_i is the occupation number of the ith state. The exchange–correlation energy $E_{\rm xc}$ is given by the local-density approximation (LDA) as

$$E_{\rm xc}^{\rm LDA} = \int {\rm d}\boldsymbol{r}\; n(\boldsymbol{r})\epsilon_{\rm xc}[n(\boldsymbol{r})] \tag{3}$$

where $\epsilon_{\rm xc}[n(\boldsymbol{r})]$ is the sum of the exchange and correlation energy per particle of a homogeneous electron gas with density $n(\boldsymbol{r})$. In the present work, we use the parametrization for $\epsilon_{\rm xc}$ of Perdew and Zunger [14].

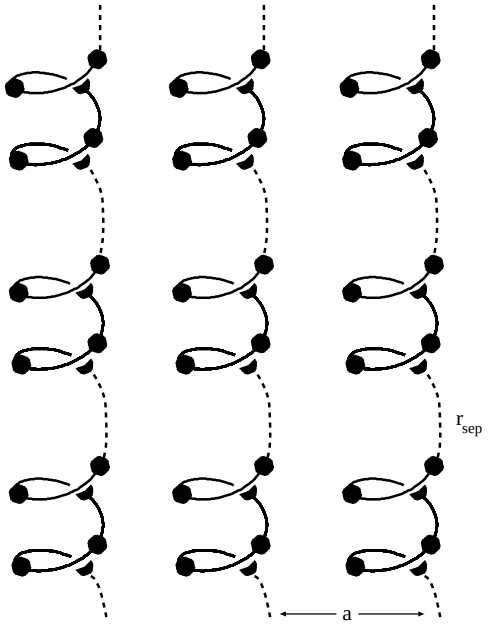

Figure 3. Our structural model, in which $r_{\rm sep}$ is the separation distance between the terminal atoms of two adjacent chains while a represents the inter-chain distance.

We calculate the total energy of the system by means of the simulated-annealing method, where we perform the annealing algorithm by the steepest-descent method. We employ the norm-conserving pseudopotential due to Bachelet, Hamann and Schlüter [15]. The simulation box is taken to be a primitive cell of the hexagonal lattice, and the energy cut-off is chosen to be 10 Ryd. In our simulations, periodic boundary conditions are adopted. The size of the simulation box is chosen appropriately for the values of the separation $r_{\rm sep}$ between the finite chains and the inter-chain distance a in figure 3. Since the accuracy of the calculations varies from size to size, comparisons of the energies are made only between the results obtained from simulations with simulation boxes of the same size.

3. What is the essential aspect?

From the experimental results explained in section 1, an actual configuration of supercritical Se is predicted to be an assembly of finite chains. Before going into detailed analyses of

three-dimensional (3D) systems, it is interesting and instructive to study one-dimensional (1D) systems. In our model system described in figure 3, this situation is realized by taking $a/a_0 = \infty$ and increasing r_{sep}/r_1 from unity, where a_0 is the interatomic distance for a crystal and r_1 is the bond length. Taking into account the fact that the inter-chain interaction is extremely small when $a/a_0 = 1.8$, we use this value in actual calculations because the situation in which $a/a_0 = \infty$ is practically realized by this value.

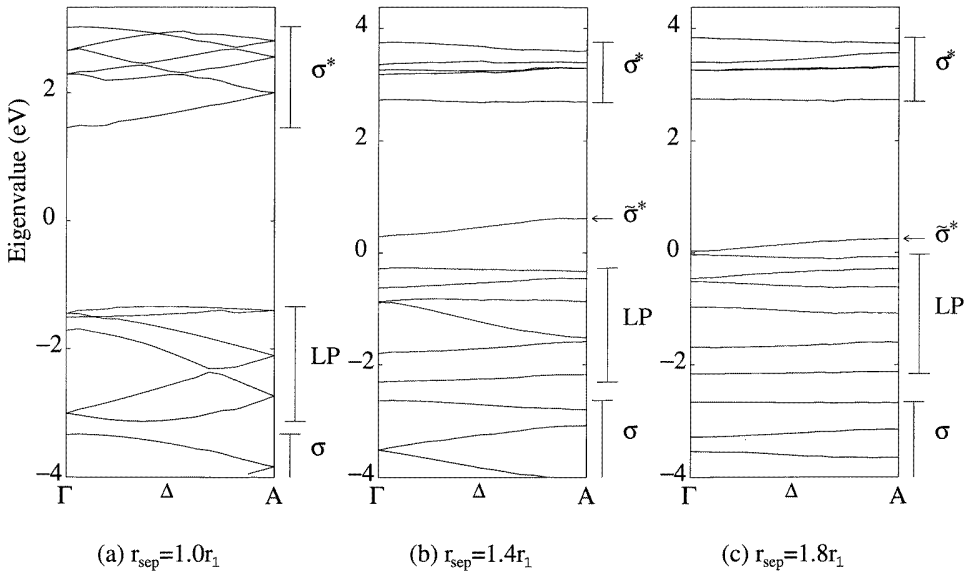

Figure 4. The band structure of a 1D assembly of helical chains of size 6 with $\phi = 120^\circ$ for the model structure illustrated in figure 3 with $a \to \infty$, and $r_{sep}/r_1 = 1$, 1.4, and 1.8.

The band structures for an assembly of threefold helical chains with size 6 are shown as solid curves in figure 4.

A remarkable point is that one out of six anti-bonding (σ^*) bands is lowered when r_{sep}/r_1 is raised from unity. When we recall our model structure as presented in figure 3 with $a/a_0 = \infty$ and $r_{sep}/r_1 > 1$, we realize that one bond out of every six in each simulation box is disrupted. As a result, the energy splitting between the bonding level and the anti-bonding level becomes smaller, and accordingly the anti-bonding band corresponding to this disrupted bond is lowered. Let us call this anti-bonding band for the disrupted bond 'the $\widetilde{\sigma}^*$-band'.

Simple though it is, this is exactly what is causing the NM-to-M transition in supercritical Se on the reduction of the density. The situation becomes clearer in succeeding sections, where we study 3D assemblies of finite helical chains.

4. What happens in 3D systems?

Motivated by the discussion about 1D assemblies of finite helical chains in the preceding section, we study 3D assemblies of finite helical chains, which are realized by taking each of the parameters r_{sep}/r_1 and a/a_0 to be a finite value larger than unity in our model shown in figure 3. Each set of r_{sep}/r_1 and a/a_0 defines a density ρ.

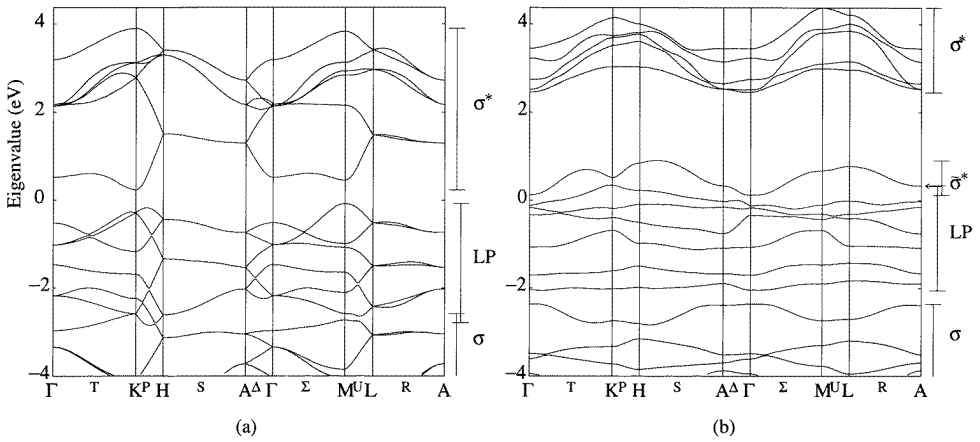

Figure 5. The band structure of a 3D assembly of helical chains of size 6 with $\phi = 120^\circ$ for the model structure illustrated in figure 3 with (a) $\rho_0/\rho = 1.3$ and (b) $\rho_0/\rho = 1.4$.

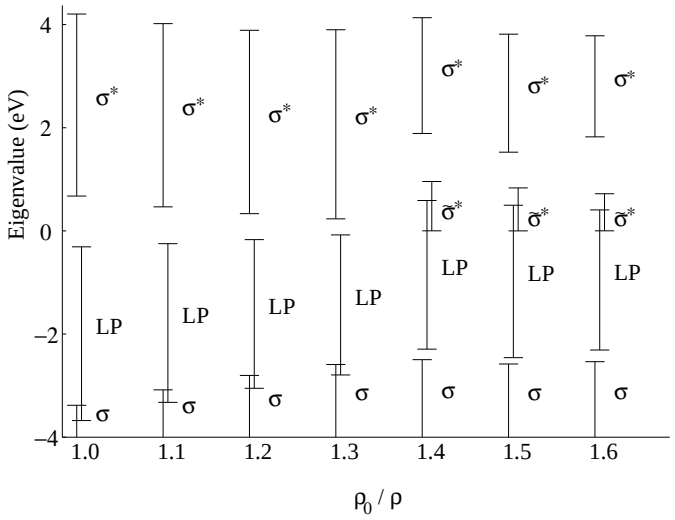

Figure 6. The energy regions for the bands versus ρ_0/ρ.

The band structures calculated for the case where $\rho_0/\rho = 1.3$ and $a/a_0 = 1.4$ are presented in figure 5. In the case where $\rho_0/\rho = 1.3$, with ρ_0 being the density for a crystal, there exists an energy gap between the highest lone-pair (LP) band and the lowest anti-bonding band ($\widetilde{\sigma}^*$), the latter being the $\widetilde{\sigma}^*$-band whose definition we introduced in the previous section. Since the Fermi level falls in this energy gap region where the density of states is zero, the system is nonmetallic.

In the case where $\rho_0/\rho = 1.4$, on the other hand, the $\widetilde{\sigma}^*$-band and the LP band are overlapping, and accordingly the system is metallic.

The energy regions for the bands are presented in figure 6. In the same way as for 1D cases, the band gap E_g decreases as ρ_0/ρ is raised from unity for a given finite value of a/a_0. When ρ_0/ρ becomes 1.4, the gap closes and the energy overlap becomes positive,

thus establishing the occurrence of a NM-to-M transition consequent upon the increase of ρ_0/ρ, or, in other words, upon the decrease of the density. The whole situation is obviously analogous to that for 1D systems.

In this way, the mechanism for the NM-to-M transition in liquid Se is proved to be the reduction of the energy splitting between the bonding (σ) level and the anti-bonding ($\widetilde{\sigma}^*$) level due to the disruption of some bonds accompanying the decrease of the density. As mentioned in the previous section, this is *the* mechanism that we have been looking for, though simple it is. A remarkable point is that the essential aspect of this mechanism is observed even in 1D systems, as fully explained in the previous section.

5. What causes bond disruption?

In order to see what causes the bond disruption in supercritical Se, we extract the essential effects of the temperature increase along the rightward arrow in figure 2(b). The relevant aspect is the decrease of the density, which causes the expansion between Se chains as well as that along the chains. We assume that the expansion is uniform in all three dimensions,

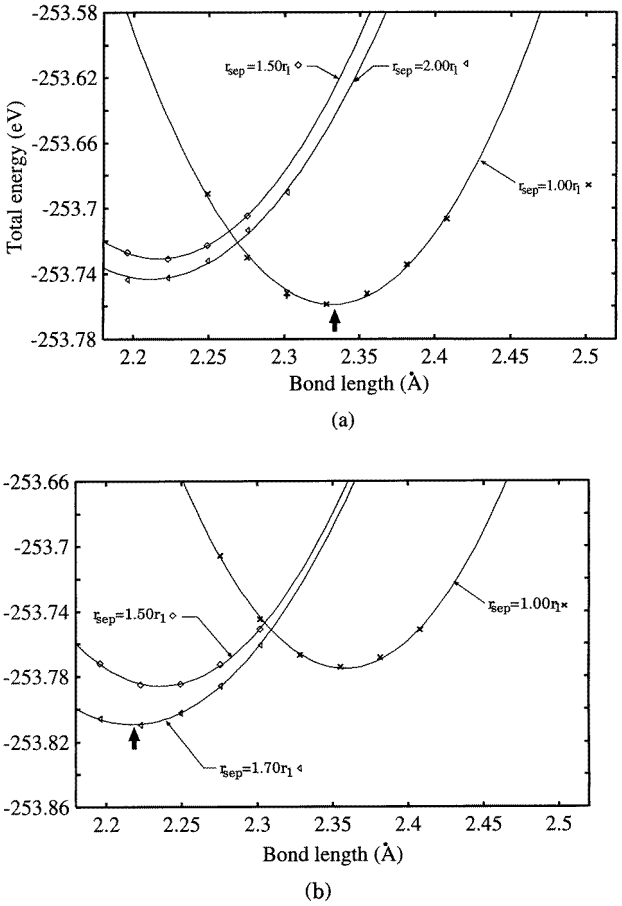

Figure 7. The total energy versus the bond length for various values of r_{sep}, where (a) $\rho_0/\rho = 1.3$ and (b) $\rho_0/\rho = 1.4$.

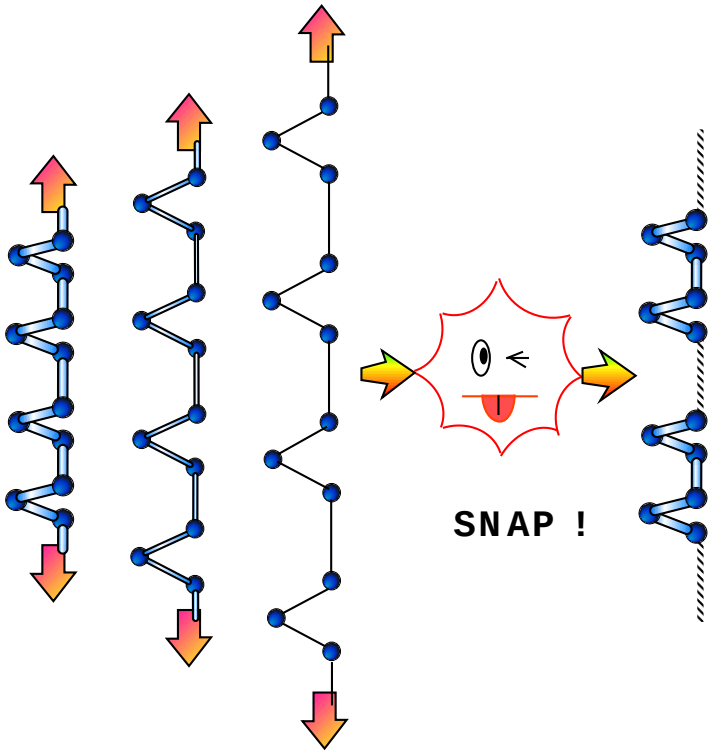

Figure 8. When a chain is stretched to a critical extent, some of the bonds are broken in order to reduce the total energy.

so the increases of $r_{\rm sep}/r_1$ and a/a_0 are both proportional to $(\rho_0/\rho)^{1/3}$.

Under this condition, we calculate the total energy as a function of the bond length for various values of ρ_0/ρ. The results are shown in figures 7(a) and 7(b), respectively, for $\rho_0/\rho = 1.3$ and 1.4. For $\rho_0/\rho = 1.3$, the lowest energy is achieved when $r_{\rm sep}/r_1 = 1$. This corresponds to an infinite chain of Se in which the bond length is the same for all bonds. For $\rho_0/\rho = 1.4$, on the other hand, the lowest energy is realized when $r_{\rm sep}/r_1$ is larger than unity.

The situation implied by these results is schematically illustrated in figure 8. When the density is decreased, the bonds are stretched from their natural length. This of course costs energy. It is worth noting, however, that, in order to avoid the stretching of the bonds, some of bonds must be disrupted. When bonds are disrupted, the gains from the bonding energies are inevitably lost. Therefore, Se atoms try to maintain all bonds even though they are stretched and the bonding energies are small.

When the density ρ is decreased, the bonds must be stretched even more. When ρ becomes lower than some marginal value, there occurs a condition where the regaining of the natural bond length at the expense of the disruption of some bonds costs less energy than a stretched chain with all bonds intact.

This is the mechanism of bond disruption. In fact, from comparison of figure 6 and figure 7, we can see that the NM-to-M transition in expanded Se is triggered by bond disruption.

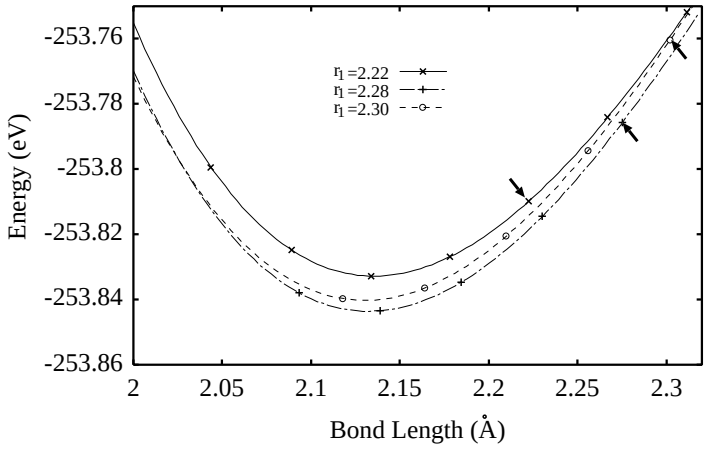

Figure 9. The energy versus the length of the terminal bonds in a finite chain.

6. What happens immediately after bond disruption?

Our calculations so far have been based on the structural model in which the bond lengths for undisrupted bonds are all the same. It is expected, however, that the lengths of terminal bonds will be different from those of internal bonds. In order to clarify this point, we calculate the total energies for various sets of the bond length, r_1, for internal bonds and that, r_1', for terminal bonds. The results of our calculations are given in figure 9. The minimum of energy is achieved for the set $r_1' = 2.14$ Å and $r_1 = 2.28$ Å. This indicates that the bond lengths of terminal bonds tend to be shorter than those of internal bonds.

These results therefore indicate that the terminal bonds are shortened when the disruption of some bonds takes place.

7. What has been shown by our work?

The conclusions obtained from our work are summarized as follows.

(i) The mechanism of the NM-to-M transition in supercritical Se is triggered by the partial disruption of bonds, which reduces the splitting between the bonding (σ) and anti-bonding (σ^*) levels as a result of density decrease.

(ii) The lengths of undisrupted bonds are decreased after the disruption of some bonds. The lengths of terminal bonds tend to be shorter than those of internal bonds.

Acknowledgments

This work was supported by a Grant-in-Aid for Scientific Research on Priority Areas 'Cooperative Phenomena in Complex Liquids' from the Ministry of Education, Science, Sports and Culture. Computer resources were kindly made available by the 'Research for the Future' Project at Keio University (JSPS-RFTF96I00102).

References

[1] Ohtani H, Yamaguchi T and Yonezawa F 1998 *J. Phys. Soc. Japan* **67** 2807
[2] Tamura K 1990 *J. Non-Cryst. Solids* **117+118** 450
[3] Tamura K 1994 *Z. Phys. Chem.* **184** 85

[4] Tamura K 1996 *J. Non-Cryst. Solids* **205–207** 239
[5] Tamura K, Inui M, Yao M, Endo H, Hosokawa S, Hoshino H, Katayama Y and Maruyama K 1991 *J. Phys.: Condens. Matter* **3** 7495
[6] Bichara C, Pellegatti A and Gaspard J-P 1994 *Phys. Rev.* B **49** 6581
[7] Hohl D and Jones R O 1991 *Phys. Rev.* B **43** 3856
[8] Kirchhoff F, Gillan M J, Holender J M, Kresse G and Hafner J 1996 *J. Phys.: Condens. Matter* **8** 9353
[9] Kirchhoff F, Gillan M J and Holender J M 1996 *J. Non-Cryst. Solids* **205–207** 924
[10] Shimojo F, Hoshino K, Watabe M and Zenpo Y 1998 *J. Phys.: Condens. Matter* **10** 1199
[11] Warren W W Jr and Dupree R 1980 *Phys. Rev.* B **22** 2257
[12] Hohenberg P and Kohn W 1964 *Phys. Rev.* **136** B864
[13] Kohn W and Sham L J 1965 *Phys. Rev.* **140** A1133
[14] Perdew J and Zunger A 1981 *Phys. Rev.* B **23** 5048
[15] Bachelet G B, Hamann D R and Schlüter M 1982 *Phys. Rev.* B **26** 4199